Study of dynamic characteristics of a new suggested recoiling mortar system

Study of dynamic characteristics of a new suggested recoiling mortar system

M Selim[1], W Elsaady[2,3], O Abdelsalam[2] and A Ibrahim[2]

[1] Technical Research Centre, Egypt
[2] Mechanical Engineering Branch, Military Technical College, Cairo, Egypt

[3] Email address: wael.elsaady@mtc.edu.eg

Abstract. The purpose of this paper is to study the characteristics of recoil motion of a new suggested recoil system designed for the Russian 120- mm PM-38 mortar, rather than the conventional fixed-barrel mortar system. The new recoil system enables to reduce the total force imparted by the mortar system to the carriage, with the purpose of the mortar can be mounted on tracked/wheeled vehicles. The paper presents the suggestion of the new recoiling mortar system along with the discussion of the presentation of constructional considerations and constraints. The dynamic characteristics of recoil motion have been modelled with the aid of a new mathematical model that have been established using MATLAB software. As a result of the suggestion of the new recoiling mortar system, the maximum recoil resistance force is predicted to be reduced by more than 60% compared to that in the traditional fixed-barrel mortar system. In addition, the maximum recoil distance was predicted to be around 26 cm.

1. Introduction

Nowadays, mounting of artillery guns on tracked/wheeled vehicles is an international ongoing research trend that has a great interest by many military armies all over the world [1]. In comparison with conventional towed artillery guns, self-propelled guns that are mounted on tracked/wheeled vehicles have better mobility, efficiency, and manoeuvrability during combat. Examples of these guns are of the CAESAR 155-mm gun developed by Nexter Company in France, the NORA B-52 155-mm gun developed by Yugoimport-SDPR Company in Serbia, and the 130-mm A-222 Bereg developed by Rosoboronexport Company in Russia.

The principle of gun recoil can be described as follows. At instant of firing, the propellant charge is burnt and generates gases with very high pressure and temperature. These gases impart massive forward impulsive force, PB to the projectile that is forced to move forward until it gets out of barrel with the required muzzle velocity. The gun barrel assembly is affected by the same impulsive force according to Newton's second law. This force is imparted directly to the gun carriage, and then to the ground, in case of fixed-barrel gun systems. Alternatively, the barrel assembly can be allowed to recoil and counter recoil by means of the "gun recoil system". This recoiling motion helps to reduce the total force imparted to the gun carriage, as shown in Figure 1. That is because the carriage will be affected by the damping resistance to the recoil motion of barrel assembly, R, rather than being affected by the force of powder gases (PB) as in fixed-barrel gun systems [2].

In principle, the gun recoil system consists of a recoil brake (RB) and recuperator (REC) [3]. The RB produces hydraulic resistance force, K, to the motion of barrel assembly. This hydraulic resistance is achieved because the RB is filled with liquid that is forced to move through narrow throttling areas

in the RB. On the other hand, the REC accumulates some of recoil energy in order to be utilized in counter recoil. This is achieved as the working medium in recuperator is either a spring or pressurized gas. Therefore, it has ability to store some of recoil energy in the form of potential energy that is represented by spring compression or gas pressure. The REC provides the main driving force of barrel assembly during counter recoil, PR. It is worth mentioning that the hydraulic resistance force has the greater contribution in the total recoil resistance, R, in comparison with recuperator force, PR and the friction force, RF which is generated due to friction in barrel guides and stuffing boxes during the recoil cycle. The direction of this friction resistance is always in opposite direction of motion of the recoiling parts. In recoiling-barrel gun systems, the gun barrel assembly is movable with respect to gun cradle, and it is connected to the two ends of the movable parts of recoil system.

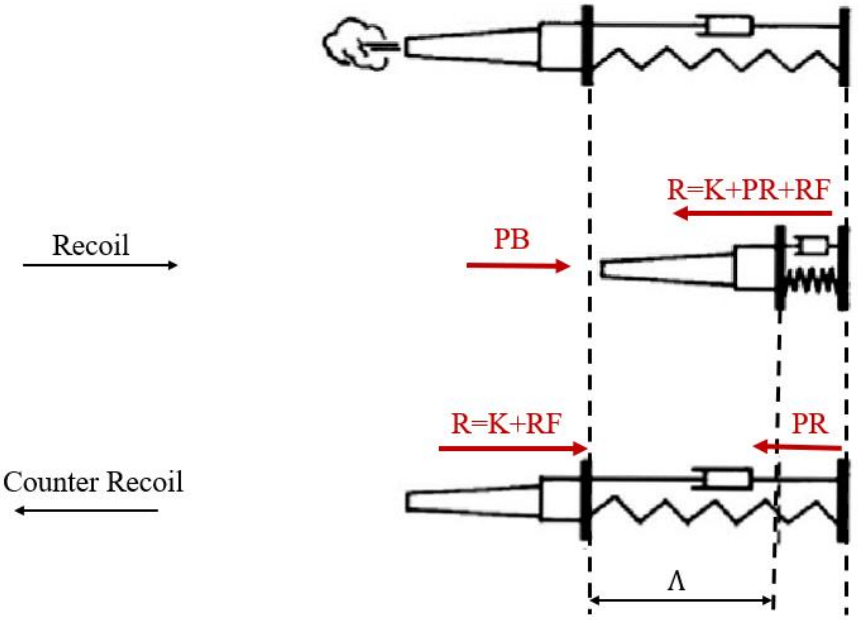

Figure 1. Gun recoil cycle.

Therefore, because of the great importance of recoiling systems in reducing the total force imparted to gun systems, researchers pay deep attention to study, analyse, and improve the characteristics of artillery recoil mechanisms. For instance, Elsaady *et al.* [4] simulated the recoil cycle of a coaxial recoil system that is used in tank guns using MATLAB/Simulink. The theoretical results give high level of confidence of the mathematical model as the results are compared with their counterparts due to real firing results. Hassaan [5] established a simulation model for the recoil cycle considering the nonlinearity of hydraulic damper and air springs to get the recoil displacement of typical Howitzer M114 155 mm cannon.

Other researchers investigated improving of recoil characteristics by different non-traditional techniques. These techniques involve the adoption of soft recoil technology and smart fluids. For example, Kang and Gimm [6] used the soft recoil technology instead of conventional recoil to improve the recoil characteristics. The principle of soft recoil mechanism allows firing when the recoiling parts that move forward reach the proper velocity level, and the forward momentum behaves against the recoil motion. Afterward, the reduction of the total recoil force and the length is expected. found that the adoption of soft recoil mechanisms leads to the reduction of maximum recoil distance by 9% as well as reduction of maximum hydraulic recoil oil pressure by 43% compared to conventional recoil. Their

results are attested by theoretical and experimental results of both recoil technologies. Akiwate and Gawade [7] investigated use of smart magnetorheological (MR) fluids rather than conventional fluids as the working fluids in gun recoil systems. They constructed a mathematical model using MATLAB/Simulink to simulate the recoil motion of the gun. It was found that using of smart fluids leads to the reduction of maximum recoil distance by 80% compared with those parameters due to employment of conventional fluids. It is worth noting that, to the best of authors' knowledge, the technology of employment of smart fluids in gun recoil systems is still in research phase, and there is no piece of guns that apply this technology up to now.

Optimization techniques are also presented in the literature in order to investigate the best design of recoil system that leads to better characteristics of recoil motion. For example, Guo [8] applied the optimization technology using BP neural network and particle swarm optimization (PSO) method for improving the maximum recoil resistance for a gun that uses soft recoil technology. The design variables of the optimization problem involved the size of throttling area of the recoil system whereas the cost function was minimization of peak value of total recoil resistance. The results are found to considerably conduce a refinement of the distribution of recoil resistance and the maximum recoil resistance value decreases by 22% of the normal design.

Regarding the available designs of recoiling mortar systems, there are very limited models of these mortars that currently existing in service in some armies. Examples of these mortars are the 120-mm ALKAR recoiling mortar. There are many design variables that can be investigated on the study of recoiling mortar systems. Examples of these parameters are the size of the variable throttling area of recoil system, mass of the recoiling parts, working area of piston, stiffness of the recuperator used, density of the working liquid in recoil system, etc.

In response to the continuous research efforts on enhancement of gun recoil systems, this paper presents (i) suggestion and design of a suitable recoil system for 120-mm mortar, with the aim of converting the current fixed-barrel mortar system into a recoiling-barrel system, and (ii) studying and evaluation of the dynamic characteristics of mortar recoil by the development of a mathematical model using MATLAB coding to simulate the gun recoil motion. The construction of the new suggested recoiling mortar is presented in Section 2, followed by the presentation of the governing equations that govern the recoil phenomenon in Section 3. After that, the results and discussions are presented in Section 4. Finally, conclusions are drawn in Section 5.

2. Construction of the new suggested recoiling mortar system

As mentioned above, the Russian 120- mm PM-38 mortar is a fixed-barrel system. The challenge in the suggestion of the new recoil system in this paper was to comply with prevention of any modifications in the barrel assembly. In other words, no machining activities are allowed in the barrel assembly. Therefore, a coaxial recoil system of the mortar has been suggested. That is because the coaxial recoil system is thought to be the best construction because of its simplicity, and the fact that the line of action of all forces affecting the mortar is the barrel axis, which is advantageous from construction point of view. The new suggested recoil system is presented by the section and 3D views of the system shown in Figure 2, Figure 3, and Figure 4, respectively. The recoiling mortar system consists of: (i) the barrel assembly of the conventional mortar system which consists of the barrel that is connected to the breech case through a thread. The firing mechanism is embedded in the breech case, (ii) the recoil system that can be described as a spring-damper system, and (iii) the connecting parts, which is coloured in blue in Figure 4, connects the recoiling piston of the recoil system with the barrel assembly. It has a cut-off part in front of firing lever to allow the function of the firing lever in the breech case. The piston is allowed to move with respect the outer cylinder that is filled with hydraulic liquid, and the liquid is forced to be throttled around the piston head. The inner guiding part provides guidance of the piston during recoil cycle. The recoil brake cylinder works as the cradle of the gun. A spring recuperator is assembled between the rear surface of the piston head and the rear end of the outer cylinder. The barrel assembly is connected to the recoil system through the connecting part. The barrel assembly, connection part, recoil brake piston, and guiding part are movable and called recoiling parts. The recoil brake

cylinder and sliding part are fixed and joined together through bolts. There are oil seals in the recoil system to prevent any leakage during the recoil cycle.

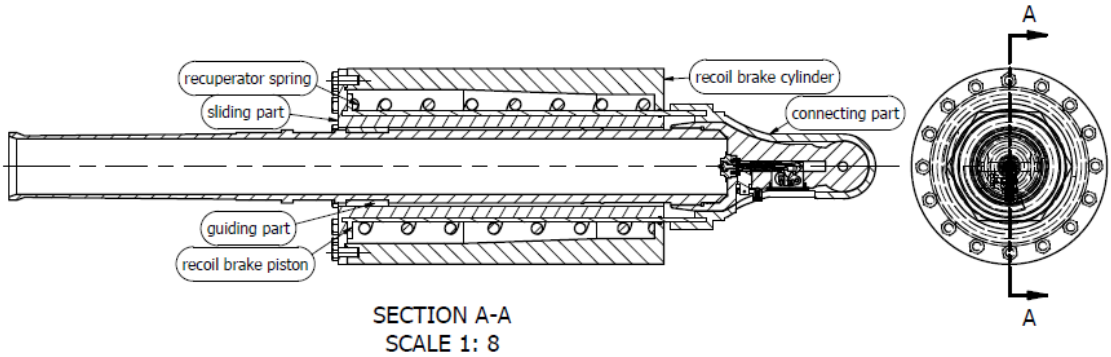

Figure 2. Sectional view of 120-mm mortar with coaxial recoil system in firing position.

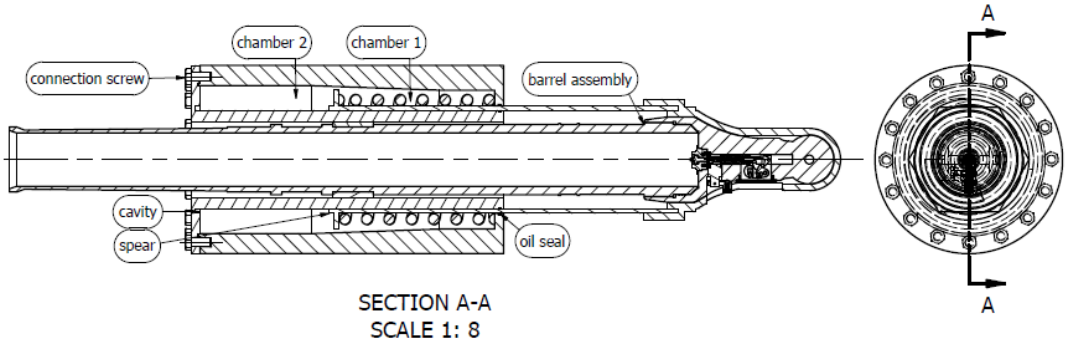

Figure 3. Sectional view of 120-mm mortar with coaxial recoil system at end of recoil motion.

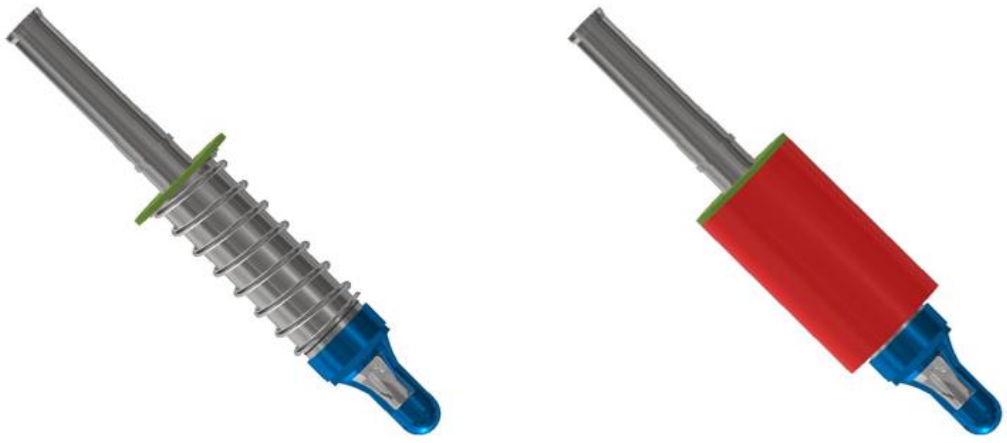

Figure 4. 3D view of 120-mm mortar with coaxial recoil system.

2.1. Function during recoil.

The position of the mortar during recoil is shown in Figure 3. When firing, force of powder gases, PB, is generated and forces the recoiling parts (the barrel assembly and the piston) to accelerate backwards.

Thus, the liquid in chamber (1) is forced to flow around piston head through the annular orifice between piston head and the inner surface of recoil brake cylinder. It should be noted that the diameter of the inner surface of recoil brake cylinder should be variable. Thereby, a requisite value of hydraulic resistance, K, along the recoil length is created. That is because the hydraulic resistance depends also on recoil velocity, as will be shown in Section 3. The spring recuperator is compressed during the recoil motion, and this evolves the recuperator resistance, PR. The summation of hydraulic resistance, K, the recuperator force, PR, and all fiction resistance to recoil motion, RF, represent the total recoil resistance, R, whose profile should be well-designed, as it represents the total force imparted to the mounting carriage of the mortar. Friction resistances are evolved due to the presence of oil seals (stuffing boxes) in the recoil system to prevent oil leakage. These stuffing boxes affect by friction force on the piston. Additional friction force is evolved due to the friction between the inner surface of piston and the outer surface of the guiding part.

Therefore, the recoiling parts move during the recoil motion under the effect of the summation of the preceding forces, namely: the force of powder gases, PB, as the main driving force, and all the aforementioned resisting forces (K, PR and RF). The recoiling parts start to accelerate as $PB > R$. When $R > PB$, the recoiling parts starts to decelerate until the end of recoil. It should be also noted that the recoil motion of the piston leads to the formation of cavitation in front of the piston. The volume of this cavitation equals to that of the protruding part of the piston during recoil.

2.2. Function during counter recoil.

The position of the mortar at the end of recoil is shown in Figure 3. At the end of recoil motion, the recoiling parts move forward under effect of the driving force stored in the spring recuperator during recoil motion. First, the cavitation formed in front of the piston during recoil vanishes. Then, the working liquid starts to flow from chamber (2) back to chamber (1). Thus, the recoiling parts continue to move forward until they reach to their initial front position. It is worth mentioning that the front part of the piston should be provided with a cushion in the form of a spear-and-cavity, as shown in figure 3. This spear-and-cavity is employed to reduce the impact that may occur at the end of counter recoil motion between the recoiling parts with the guiding cylinder (cradle). In other constructions of gun recoil systems, this braking can be provided by stand-alone systems that are often called as “counter recoil brakes”.

3. Mathematical model

The mathematical model is based on the study of the equation of motion of recoiling parts of the mortar during recoil. The equation of motion when firing at maximum elevation angle can be written as shown by equation (1).

$$M_{R_i} a_i = PB_i - K_i - PR_i - RF_i + Q_R \, sin(\varphi_{max}) \tag{1}$$

where M_R is the mass of recoiling parts, a is the acceleration of recoiling parts, Q_R is the weight of recoiling parts, and φ_{max} is the maximum elevation angle.

The choice of studying of the recoil motion when firing at maximum angle is because the component of recoiling parts weight in the direction of recoil, $\mathrm{Q_R}\sin(\varphi_{\max})$, has its maximum value. This leads to greater value of driving force. The mathematical model has been established using MATLAB software in order to apply integration of equation (1) so that the histories of recoil velocity,V, and recoil distance, X, can be determined. To do this, there is a need to model all the driving and resisting forces seen in equation (1), namely: the force of powder gases, PB, hydraulic resistance, K, recuperator force, PR, and fiction resistances, RF. It should be noted that some of these forces are functions of the recoil parameters,V, and X So, numerical integration has been applied to equation (1) using MATLAB software. Therefore, in the following subsections, the governing equations of driving and resisting forces will be presented.

3.1. Force of powder gases

It should be taken in consideration that the recoil motion has three main periods as following:

- Period I: Starts from ignition instant until the instant whenever the projectile leaves the gun muzzle. At which recoiling masses include the mass of projectile and propellent also.
- Period II: Starts from muzzle point until instant of end of additional action of powder gases (AAPG).
- Period III: Starts from end of AAPG to the end of recoil motion.

The force of powder gases produces the driving impulse to the recoiling parts, and it affects only in Period I and II. In Period I, the force of powder gases can be determined from the variation of gas pressure inside the barrel that is determined from internal ballistics (IB) solution. The Charbonier-Sugot model that has been used to solve the IB parameters [9]. In Period II, the pressure drop is determined by the solution of gas expansion process during this period, from which the variation of pressure can be determined. The governing equation that governs the variation of pressure during this period is the well-known Bravin's equation, as shown by equation (3) and Figure 5.

$$p_i = p_M * e^{-\frac{t_i - t_M}{b}} \tag{2}$$

where p_M is the pressure at muzzle point, t_M time period taken until muzzle point, and b is the Bravin's coefficient.

$$PB_i = p_i * S \tag{3}$$

where S is cross section area of barrel.

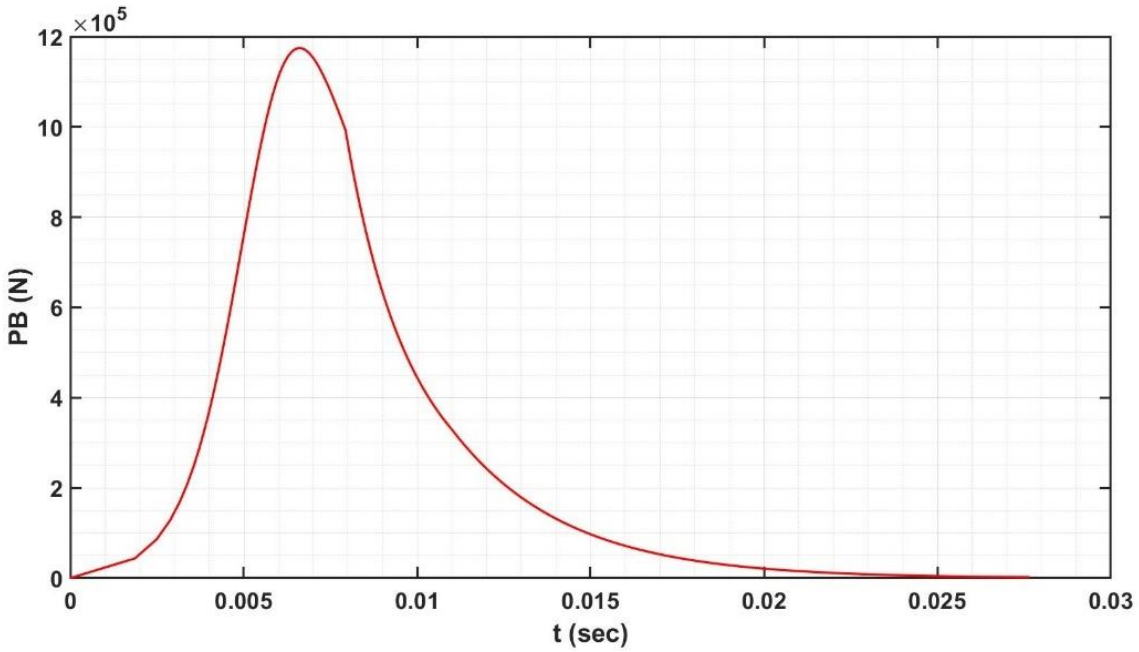

Figure 5. Force of powder gases VS time.

3.2. Friction resistances

The friction resistance occurs due to the friction in barrel guide part and the inner surface of sliding part besides the friction in stuffing boxes of recoil system. The friction resistance can be represented by equation (4).

$$RF_i = Q_R \,.\, (f \,.\, co\, s(\varphi_{max}) + \upsilon) \tag{4}$$

where f is the friction coefficient between guiding part and cradle, and υ is friction coefficient in stuffing boxes of recoil system.

3.3. Recuperator force

The recuperator force due to compression of spring recuperator during recoil can be represented by equation (5). The recuperator force should have an initial value, PR_O. This force secures returning the mortar recoiling parts to their initial position after recoil.

$$PR_i = PR_O + KS \,.\, X_i \tag{5}$$

where KS is the spring stiffness.

3.4. Hydraulic resistance

In order to determine the expression of hydraulic resistance, the flow of liquid inside recoil brake cylinder is studied by applying the continuity and modified Bernoulli's equations. Therefore, the variation of pressure difference between Chamber (1) and (2) with time can be determined, as shown by equation (6).

$$K_i = \left(p_{1_i} - p_{2_i}\right).A_{PB} \tag{6}$$

where p_1, p_2 are the pressures in chamber (1) and (2) respectively, and A_{PB} is the working area of piston during recoil motion.

3.4.1. Continuity equation. To apply continuity equation for the flow of liquid inside the recoil system, the flow parameters are studied at two points along the streamline of the flow. The continuity equation can be written as:

$$v_{f2_i} = \frac{APB + A_i}{A_i} \,.\, \frac{1}{\propto_2} \,.V_i \tag{7}$$

where v_{f2} are the velocity of flow in section 2, and $\propto_2$ is the contraction coefficient of flow through throttling orifices.

3.4.2. Bernoulli's equation. The Bernoulli's equations can be determined, as shown by equation (8) under the following assumptions: (i) steady-state flow in the recoil system, (ii) incompressible fluid, (iii) one-dimensional flow, and (iv) friction losses depend only on fluid velocity.

$$p_{1_i} + \frac{\rho_l \,.\, {v_{f1_i}}^2}{2} = p_{2_i} + \frac{\rho_l \,.\, {v_{f2_i}}^2}{2} + \xi_2 \,.\, \frac{\rho_l \,.\, {v_{f2_i}}^2}{2} \tag{8}$$

$$v_{f1_i} = 0 \tag{9}$$

$$p_{1_i} - p_{2_i} = (1 + \xi_2).\, \frac{\rho_l \,.\, {v_{f2_i}}^2}{2} \tag{10}$$

where v_{f1} are the velocity of flow at Point 1 (in Chamber 1 behind the piston head), ρ_l is the recoiling liquid density, and ξ_2 is the coefficient of friction and local losses.

By the substitution for (v_{f2_i}) from equation (7) into equation (10), the pressure difference between Chamber (1) and (2) can be determined as follows:

$$C_2 = \frac{\rho_l}{2} \,.\, \frac{1+\xi_2}{{\propto_2}^2} \tag{11}$$

$$p_{1_i} - p_{2_i} = C_2 \,.\, (\frac{APB+A_i}{A_i})^2 \,.V_i{}^2 \tag{12}$$

Therefore, the hydraulic resistance, K, can be determined as follows:

$$K_i = C_2 \,.A_{PB} \,.\, (1 + \frac{APB}{A_i})^2 \,.V_i{}^2 \tag{13}$$

Therefore, by having the expressions of force of powder gases, equation (2), friction resistance, equation (4), recuperator force, equation (5), and hydraulic resistance force, equation (13), the recoil parameters can be determined using equation (1). As a first step of design, the variation of total recoil resistance with time, R, and some other parameters are first assumed. Hence, the requisite profile of hydraulic resistance, K, is determined, and consequently the profile of the throttling area of recoil system according to the following equation.

$$A_i = \frac{A_{PB}}{\sqrt{\frac{K_i}{C_2 * APB * V_i{}^2} - 1}} \tag{14}$$

The profile of the throttling area of recoil system determined from equation (14) cannot be machined using traditional methods of machining such as turning and milling operations. Therefore, the profile of the throttling area is modified so that it can be implemented with these common methods. Therefore, the same model is used to determine the actual recoil parameters, namely: recoil resistance, R, recoil velocity, V, and recoil distance, X.

3.5. Selection of the requisite total recoil resistance

The profile of total resistance has been assumed to start with a value (R_O = 9.5161 KN). Then, it increases linearly until the instance of maximum pressure inside barrel, at which the value is assumed as ($R_{Pmax} = 250\ KN$), at which it remains constant until the moment of end of AAPG. After that, the total recoil resistance decreases linearly to reach value ($R_\Lambda = 18.516$ KN) at the end of recoil motion. The values of R_O and R_Λ depend only on recuperator and fiction resistances, as there is no hydraulic resistance since the recoil velocity is zero. The variation of the requisite total recoil resistance is shown in Figure 6.

The calculations of recoil dynamic characteristics based on equation of motion in two steps (i) determination of free recoil parameters, which means recoil dynamic characteristics whilst there is no resistance force (ii) determination of the braked recoil parameters, which means recoil dynamic characteristics when presence of recoil forces.

3.5.1. Free recoil calculation. The free recoil characteristics of velocity (W_i) and the displacement (L_i) are determined as follows.

I. The free recoil characteristics in the period I can be calculated as follows:

$$W_i = \frac{m_p + 0.5 m_w}{m_R + m_p + m_w} \times v_{p_i} \tag{15}$$

$$L_i = \frac{m_p + 0.5 m_w}{m_R + m_p + m_w} \times x_{p_i} \tag{16}$$

where v_p , x_p , and m_p are the projectile velocity, travel, and mass respectively, and m_w is the propellent mass.

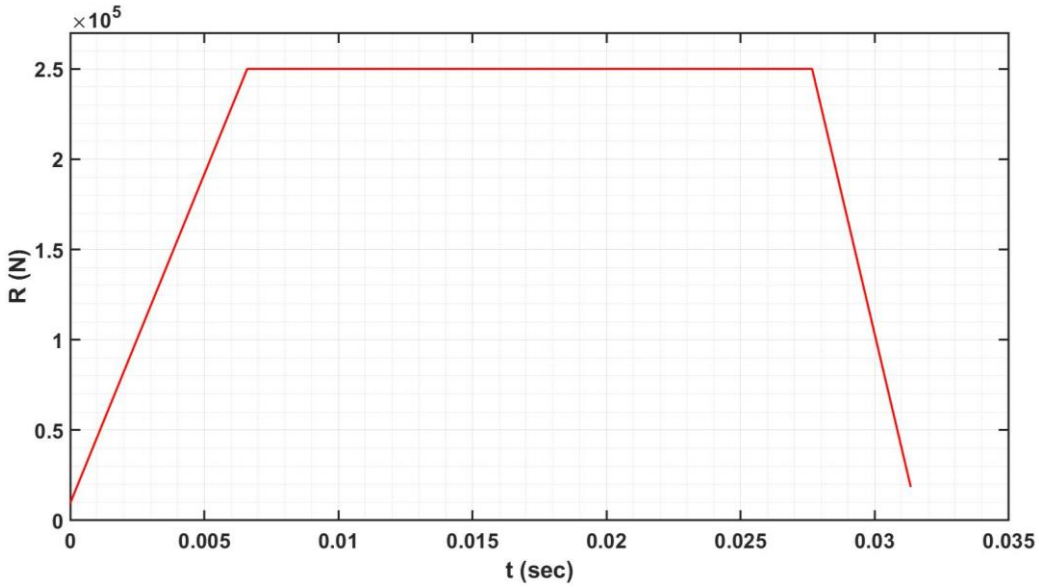

Figure 6. Requisite total recoil resistance VS time.

II. The free recoil parameters in the period II can be calculated as follows:

$$W_i = W_M + \frac{1}{m_R}.P_M.b.\left(1 - e^{-\frac{t-t_M}{b}}\right) \quad (17)$$

$$L_i = L_M + W_M.(t - t_M) + \frac{1}{m_R}.P_M.b.\left((t - t_M) - b\left(1 - e^{-\frac{t-t_M}{b}}\right)\right) \quad (18)$$

where W_M and L_M are free recoil velocity and distance at muzzle point.

3.5.2. Determination of braked recoil parameters. The recoil period is divided into 4 periods, namely: period of projectile motion until (Pmax), period of projectile motion from (Pmax) till muzzle point, period from muzzle point until end of AAPG, and Period from end of AAPG until the end of recoil. The braked recoil velocity (V_i) and the braked recoil distance (X_i) are determined as follows:

I. Period of projectile motion until Pmax

$$V_i = W_i - \frac{1}{m_R+m_P+m_\omega}\left(R_o + \frac{R_i-R_o}{2t_{p_{Max}}} * t_i\right) * t_i \quad (19)$$

$$X_i = L_i - \frac{1}{m_R+m_P+m_\omega}\left(R_o + \frac{R_i-R_o}{3t_{p_{Max}}} * t_i\right) * \frac{{t_i}^2}{2} \quad (20)$$

II. Period of projectile motion from P_{max} until muzzle point

$$V_i = V_{p_{max}} + (W_i - W_{p_{max}}) - \left(\frac{R_M}{m_R+m_P+m_\omega}\right).(t - t_{p_{Max}}) \quad (21)$$

$$X_i = X_{i-1} + \frac{V_i+V_{i-1}}{2} * (t_i - t_{i-1}) \quad (22)$$

III. period from muzzle point until end of AAPG.

$$V_i = V_M + \frac{1}{m_R}.P_M.b.(1 - e^{-\frac{t_i - t_M}{b}}) - \frac{R_{EA}}{m_R}.(t_i - t_M) \quad (23)$$

$$X_i = X_M + V_M * (t_i - t_M) + \frac{1}{m_R}.P_M.b.((t_i - t_M) - b.(1 - e^{-\frac{t_i - t_M}{b}})) - \frac{R_{EA}}{2.m_R}.(t_i - t_M) \quad (24)$$

IV. Period from end of AAPG until the end of recoil.

$$t_{II} = \frac{2.m_R.V_{EA}}{R_{EA} + R_A} \quad (25)$$

$$V_i = V_{EA} - \frac{1}{m_R}\left(R_{EA} - \frac{R_{EA} - R_A}{2t_{II}} * (t_i - t_{EA})\right) * (t_i - t_{EA}) \quad (26)$$

$$X_i = X_{EA} + V_{EA} * (t_i - t_{EA}) - \frac{1}{m_R}\left(R_{EA} - \frac{R_{EA} - R_A}{3t_{II}} * (t_i - t_{EA})\right) * \frac{(t_i - t_{EA})^2}{2} \quad (27)$$

4. Results.

The results of theoretical and modified mathematical model focus on the dynamic characteristics of recoil motion. This includes the presentation of time histories of recoil velocity and distance, variation of throttling area, and total recoil resistance.

The variation of theoretical throttling area and its modification of recoil system with recoil distance are represented in Figure 7. Modification of throttling area profile is assumed to start constant and has the value of peak value of theoretical throttling area till recoil distance 0.1m, then decreases linearly reaching a value $0.0012\ m^2$.

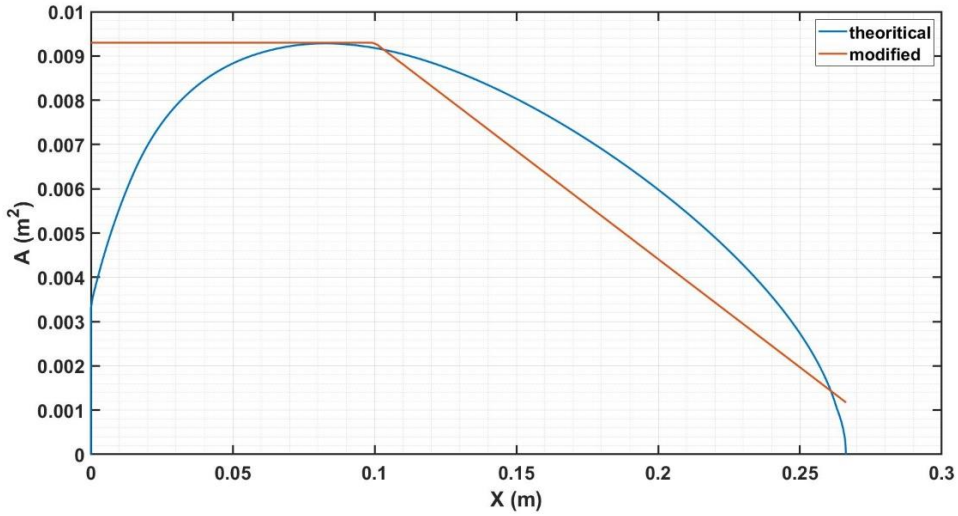

Figure 7. Theoretical and modified throttling area VS recoil distance.

The theoretical and modified variation of total recoil resistance of recoil system with recoil time are shown in Figure 8. It is seen that the modification suggested leads to a considerable increase in peak value of the total recoil resistance. This increase is compulsory because the profile of the theoretical throttling area has been assumed on the basis of an ideal distribution of total recoil resistance. However, this ideal profile of throttling area cannot be attained by traditional machining methods. Therefore, the

irregular distribution of recoil force due to the modified throttling is predicted. This heightens the need for applying optimization techniques in order to determine the best profile of recoil resistance area that leads to best distribution of recoil force.

The theoretical and modified variation of recoil velocity of recoiling parts with recoil time is shown in Figure 9. The velocity profile for both is normal but the maximum value of recoil velocity is higher than their values in and that is due to the heavy weight of barrel assembly for mortar than heavy guns.

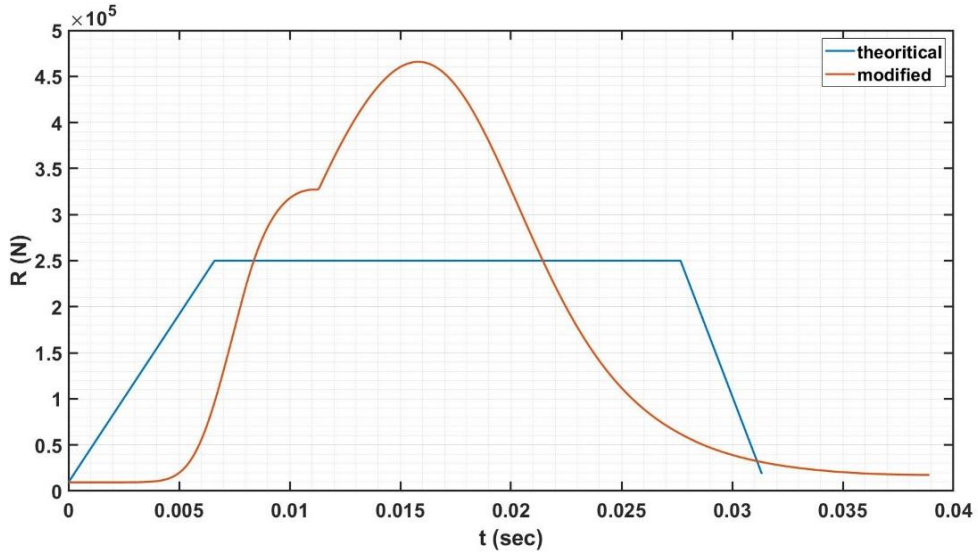

Figure 8. Theoretical and modified total recoil resistance VS time.

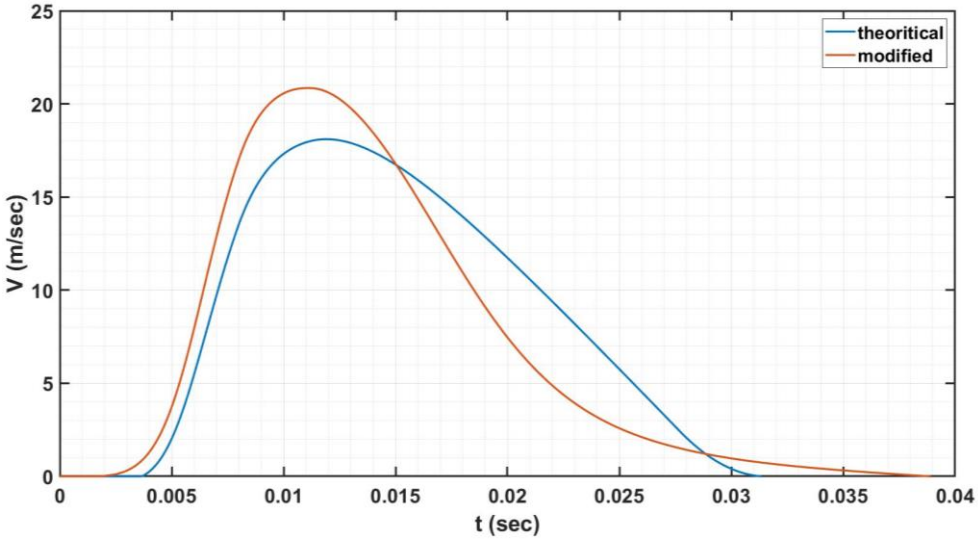

Figure 9. Theoretical and modified recoil velocity VS time.

The theoretical and modified variation of recoil distance of recoiling parts with recoil time is shown in Figure 9 It is seen that both profiles of the throttling area lead to approximately the same value of maximum recoil length. However, the modified profile leads to relatively longer recoil time. This is also because that the theoretical profile is based on an ideal distribution of recoil force whose corresponding profile of throttling area cannot be machined with conventional machining methods.

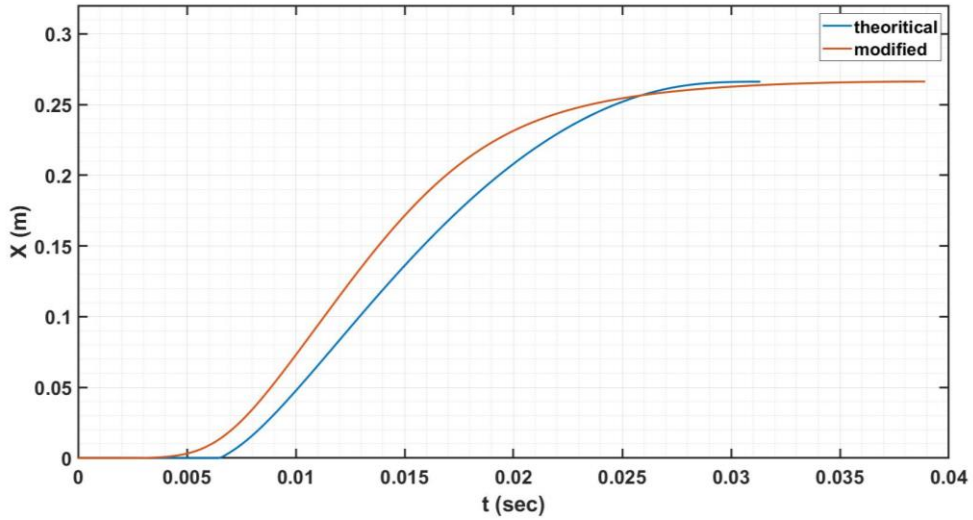

Figure 10. Theoretical and modified recoil displacement VS time.

5. Conclusions

- This paper presents a novel idea for the inclusion of a recoil system in the conventional fixed-barrel Russian mortar.
- The established modification is better as it based on a machinable throttling area that can be suitable for production.
- The recoil motion time after modification of throttling area will increase from 32 to 39 milliseconds which can be neglected.
- The recoil distance still constant despite of modification as shown in Figure 10 and has a value of 266.2 mm.
- The course of total recoil resistance distribution become different as shown in Figure 8 . the max recoil resistance increases from 25 ton to 47 ton.
- According to the change of total recoil resistance, the recoil velocity distribution is also change as shown in Figure 9 and the value of max recoil velocity of recoiling parts increases from 18 to 21 m/s.
- The model results after modification of throttling area are satisfactory but are needed to be improved.
- The future work aims to decrease the max total recoil force and the recoil distance therefore, optimization theory will be used.
- Multi-objective genetic algorithm (MOGA) based on response surface will be used to improve these characteristics of the recoil motion to get the optimum recoil input parameters and output characteristics.

References

[1] Shen Q-m, Wang G-b, Zhao J-z, Meng C, Yuan Y-q and Wang E-l 2023 Summary and Prospect of Artillery Recoil Reduction Technology. In: *Journal of Physics: Conference Series*: IOP Publishing) p 012051

[2] Miao W, Qian L and Chen L 2022 Hydraulic node model and parameter identification of a dull recoil brake *Journal of Mechanical Science and Technology* 1-11

[3] Lin T Y, Ping H C, Yang T Y, Chan C T and Yang C C 2009 Dynamic simulation of the recoil mechanism on artillery weapons. In: *ICCES*, pp 115-21

[4] Elsaady W, Abd Allah A, Ibrahim A and Hussien A 2014 Dynamic Simulation of Tank Gun Recoil Cycle. In: *The International Conference on Applied Mechanics and Mechanical Engineering*: Military Technical College) pp 1-11
[5] Hassaan G A 2014 On Dynamics of a Cannon Barrel-Recoil Mechanism with Nonlinear Hydraulic Damper and Air-Springs *IJRIT International Journal of Research in Information Technology* **2** 704-14
[6] Kang K and Gimm H 2012 Numerical and experimental studies on the dynamic behaviors of a gun that uses the soft recoil system *Journal of mechanical science and technology* **26** 2167-70
[7] Akiwate D C and Gawade S S 2014 Design and performance analysis of smart fluid damper for gun recoil system *International Journal of Advanced Mechanical Engineering* **4** 543-50
[8] Guo S-q 2020 Simulation and Parameters Intelligent Optimization of Soft Recoil System. In: *2020 Chinese Automation Congress (CAC)*: IEEE) pp 3663-8
[9] Rao K S and Sharma K C 1981 Art in Internal Ballistics *Defence Science Journal* **132** 157-74